Field Testing of a Model for Water Flow and Heat Transport in Variably Saturated, Variably Frozen Soil

XIA XU, JOHN L. NIEBER, JOHN M. BAKER, AND DAVID E. NEWCOMB

The simultaneous heat and water (SHAW) model was tested with soil water content and temperature profile data for a soil located near Rosemount, Minnesota. The predicted frost-thaw depth, soil water content, and temperature at depths of 10, 20, and 80 cm are compared with measured values. The results indicate that the prediction of frost depth and temperature profile agrees well with measured field data, whereas agreement between measured and predicted liquid soil water content is fair. The model was applied to a hypothetical case of a paved soil to assess the impact of the presence of the pavement on frost penetration into the soil profile. It was found that the frost front penetrates deeper into the underlying soil in the case of a paved soil surface in contrast to the case of an unpaved soil.

Seasonal freezing and thawing of soil occurs in a large part of the earth's land mass. Freezing-thawing phenomena affect many natural processes and have a significant influence on many human activities. The study of heat and water transfer, freezing, and thawing has been involved in many disciplines including agriculture, hydrology, civil engineering, environment, and geology. Extensive reviews of current knowledge associated with heat and mass transfer and the effects on soil physical properties were prepared by Czurda (*1*), Kay and Perfect (*2*), and Lundin (*3*). Since the early 1970s, numerous papers have been written on the modeling of simultaneous transport of heat and water in soils subjected to freezing and thawing (*3–18*).

The freezing-thawing process influences many soil properties including hydraulic, thermal, and physical strength properties, and therefore the process affects not only the transport of heat and water but also the strength of the soil. In the natural environment, the freezing-thawing process affects the partitioning between infiltration and runoff of snowmelt and rainfall (*3*), and therefore it has a major impact on runoff generation and soil erosion (*15,19*). The process also influences the redistribution of soil water (*20,21*) during the winter months and will thereby affect the magnitude and temporal distribution of groundwater recharge.

The processes of soil freezing and thawing can dramatically affect the stability of manmade structures such as building foundations, retaining walls, and highway pavements (*22,23*). Although the freezing of the soil can increase the mechanical strength of the soil, frost heaving might accompany the freezing process resulting in severe structural damage (*24*). Even when frost heaving does not occur, the thawing of a previously frozen soil can drastically reduce the mechanical strength of the soil during the thawing period.

The modeling of simultaneous heat and water transport in soils subjected to cycles of freezing and thawing temperatures can improve the understanding of the effects of soil and climate parameters on the water and temperature status of soils. The modeling process facilitates the prediction of trends in the outcome for the system prior to construction of the system and therefore can provide alternative strategies for establishing design criteria (*25*).

One model of simultaneous water and heat transport that incorporates freezing/thawing conditions is the SHAW model presented by Flerchinger and Saxton (*15*). This model is a physically based model originally designed for application in an agricultural field, soil-crop, residue-snow system, and is capable of predicing soil temperature, liquid soil water content, ice content, soil solutes distribution, and freezing and thawing depth. Because of its physical basis and flexibility for model input parameters, the model may be applied to other conditions like highway pavement.

The objectives of the study are to (a) test and evaluate the SHAW model with measured field data and (b) apply the model to the condition in which a pavement is present to assess the effect of the pavement on the frost and thaw depth in soil.

GOVERNING EQUATIONS FOR MASS AND HEAT TRANSPORT

For an unsaturated soil under freezing conditions, three phases are present in the system, including solid (soil particles and ice), liquid (unfrozen water), and gas (air and water vapor). The time-dependent status of each of the phases can be described by equations for conservation of mass and energy along with constitutive relations describing fluxes of heat and mass. The flow of water occurs in two phases, the liquid and vapor phases. For the flow of water in each of the two phases, the driving forces consist of both the hydraulic gradient and the temperature gradient (*26,27*). The temperature gradient induces the flow of water both in liquid water and in vapor phases. The flowing liquid water and water vapor carry heat and thereby affect the temperature gradient.

X. Xu and J. L. Nieber, Department of Agricultural Engineering, University of Minnesota, 1390 Eckles Avenue, St. Paul, Minn. 55108. J. M. Baker, USDA-ARS and Soil Science Department, University of Minnesota, 1991 Upper Buford Circle, St. Paul, Minn. 55108. D. E. Newcomb, Civil and Mineral Engineering Department, University of Minnesota, 18 East 49th Street, Minneapolis, Minn. 55414.

Early work regarding the mathematical description of coupled flux laws for water and heat was done by Philip and de Vries (*26*), de Vries (*27*), and Taylor and Cary (*28*). These works have led to the definition of two distinct approaches for deriving the constitutive relations for coupled water flow and heat transport in porous media. Hillel (*29*) refers to these approaches as the mechanistic approach represented by Philip and de Vries (*26*), and the irreversible thermodynamic approach represented by Taylor and Cary (*28*). The main difference between these two approaches lies in the definition of the coefficients appearing in the constitutive relations.

The SHAW model has essentially adopted the mechanistic approach to simulate heat and water transport in freezing soil. In deriving the governing equations, it is assumed that the change in fluid storage because of the compressibility of the soil and water is negligible compared to that because of the change in saturation of the soil (which is true for natural flow conditions), and that liquid water transport in response to thermal and osmotic gradient is negligible. The water balance equation for a variably saturated, variably frozen, vertical soil profile is Equation 1, and the heat balance is Equation 2, after neglecting the heat content change caused by the sensible heat flux by vapor flow (*14*).

$$\frac{\partial \theta_l}{\partial t} + \frac{\rho_i}{\rho_l}\frac{\partial \theta_i}{\partial t} = \frac{\partial}{\partial z}\left[k\left(\frac{\partial \Psi_m}{\partial z} - 1\right)\right] - \frac{1}{\rho_l}\frac{\partial q_v}{\partial z} + \frac{1}{\rho_l}S_w \qquad (1)$$

$$C\frac{\partial T}{\partial t} - \rho_i L_f \frac{\partial \theta_i}{\partial t} + L_v\left(\frac{\partial \rho_v}{\partial t} + \frac{\partial q_v}{\partial z}\right) = \frac{\partial}{\partial z}\left(\lambda \frac{\partial T}{\partial z}\right) - c_l\frac{\partial (q_l T)}{\partial z} + S_h \qquad (2)$$

where

θ_l = volumetric liquid water content, m^3/m^3;
t = time, sec;
ρ_i = density of ice, kg/m^3;
ρ_l = density of liquid water, kg/m^3;
θ_i = volumetric ice fraction, m^3/m^3;
k = unsaturated hydraulic conductivity, m/sec;
Ψ_m = soil matric potential, m;
z = depth from soil surface, m;
q_v = flux of water vapor in the z direction, kg/m^2-sec;
S_w = source or sink term for liquid water, kg/m^3-sec;
C = apparent volumetric heat capacity of soil, J/m^3-°C;
T = soil temperature, °C;
L_f = latent heat of fusion, J/kg;
L_v = latent heat of vaporization, J/kg;
ρ_v = density of ice, kg/m^3;
λ = thermal conductivity of the soil, W/m-°C;
c_l = heat capacity of liquid water, J/kg-°C;
q_l = flux of liquid water in z direction, kg/m^2 sec; and
S_h = heat source or sink term, W/m^3.

Flerchinger (*14*) used the finite difference method with the Newton-Raphson iterative technique to solve the simultaneous heat and water equations given by Equations 1 and 2 for the soil. Similarly, the governing equations for water flow and heat transport in the snowpack and in the crop residue layer were developed and solved using the same numerical method.

Boundary and Initial Conditions

The conditions at the upper boundary drive the flow of water and transport of heat within the soil profile. The heat and water fluxes between the atmosphere and the soil system are calculated on the basis of energy and mass balance between the atmosphere and the soil system. The heat balance at the upper boundary is composed of heat conduction into the surface, latent heat, and sensible heat transfer into the atmosphere. The water balance for the upper boundary is composed of precipitation, snowmelt, water flux into the surface by infiltration, evaporation, and surface runoff. Therefore, the heat and water balance at the upper boundary contains the coupled processes of water flow and heat transport. The heat and water balance can be derived with commonly available weather data.

For a paved surface, the vapor flux from the surface to the air or water flux from the air into the surface is small because of the low hydraulic conductivity of the pavement. Because of this low flux rate, the energy consumption by the latent heat flux will be insignificant.

In the SHAW model, the lower boundary conditions for the heat and water equations are taken to be specified temperature and soil water content, respectively. These specified values can be either a constant with time or varying with time. The initial conditions for the SHAW model are specified temperature and soil water content in the soil profile for the heat equation and water equation, respectively. Weather variables are applied on hourly basis.

SHAW MODEL INPUT-OUTPUT FILES

Because of model availability and its physical basis, the SHAW model was selected for testing with the measured field data in this study. The model requires input data for the following five files: (a) the description of input and output data files; (b) hourly weather data including air temperature, wind speed, relative humidity, solar radiation, and precipitation; (c) soil temperature profile; (d) the soil water content profile; and (e) description of the site characteristics. For the third and fourth files, at least two profiles are required for the initial profile and for the profile at the end of the simulated period.

The site characteristic file requires information including the simulation period, location, slope, and aspect of the study site, albedo of dry soil, and some aerodynamic roughness parameters. It also facilitates specification of up to 20 layers for the soil, and corresponding soil texture and other physical properties for each layer. If snow, crop-residue, or a solute are present in the system, additional information is required for each of their corresponding properties.

Output of the SHAW model yields nine files including (a) general output information and hourly or daily temperature, soil water, and solute profiles; (b) side-by-side predicted and measured soil water and temperature profiles; (c) predicted temperature profiles; (d) predicted soil water profiles; (e)

water balance summary; (f) frost/thaw depth and ice content profile; (g) summary of energy flux at the upper boundary; (h) total solute concentration profiles; and (i) solute concentration of soil solution.

SHAW MODEL TESTING

In this study, the SHAW model was tested using a set of measured field data including weather data, soil property data, and measured liquid soil water content and temperature profiles for an agricultural experimental field located in Rosemount, Minnesota. Then using the same weather data and soil profile data, two simulations were performed, one for a paved surface and the other for an unpaved surface. Results are presented in the form of three simulation runs. Run 1 is for an instrumented agricultural field with a bare soil surface; this run is referred to as the unpaved field site. The lower boundary conditions for soil temperaure and soil water content in Run 1 are measured soil temperature and measured soil water content at a depth of 1 m. The simulation results in Run 1 were used to compare profiles of soil temperature, liquid soil water content, and frost-thaw depth predicted with the SHAW model with field measurements of the same variables.

All information for Run 2 was the same as in Run 1 except the lower boundary was defined at a depth of 10 m, where soil temperature was considered as constant over a year. Soil water content was also specified to be a constant throughout the period of simulation at this depth. Run 3 is for the hypothetical highway pavement profile, which differs from Run 2 in replacing the top 40 cm of soil in the unpaved soil profile with 25 cm of concrete and 15 cm of base coarse material. The pavement and subsurface conditions in Run 3 are similar to the conditions at an instrumented field site near Faribault, Minnesota. The simulated results presented by Runs 2 and 3 are used to assess the effect of the paved surface on frost-thaw depth.

Unpaved Field Site Description

The data acquisition site for the field testing of the SHAW model is located at the Agricultural Experiment Station in Rosemount, Minnesota. The slope of the land is essentially zero. The land is cultivated and the top 20 cm was considered as the tilled layer. There was no crop residue cover on the soil surface during the period of data acquisition. A plan view of the site is shown in Figure 1. A weather station at the site measured incoming solar radiation, precipitation, air temperature, relative humidity, and wind speed. Total soil water content was measured with the neutron scattering method, while liquid soil water content was measured with the method of time domain reflectometry (TDR) (*30,31*). Soil temperature was measured with copper-constantan thermocouples. The sensors for measuring temperature and liquid soil water content were installed at depths of 2.5, 5, 10, 20, 30, 40, 60, 80, and 100 cm.

The required initial soil water content and temperature profiles for Run 1 were measured and are shown in Figure 2. The required lower boundary conditions at 1-m depth for

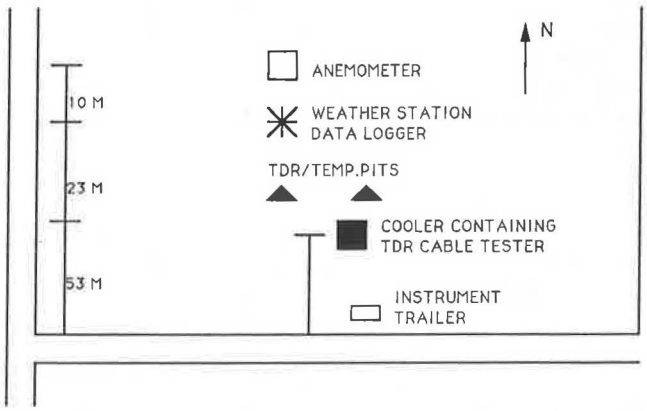

FIGURE 1 Plan view of the site for acquisition of weather data, soil temperature profile data, and soil water content profile data located at the Rosemount Experiment Station.

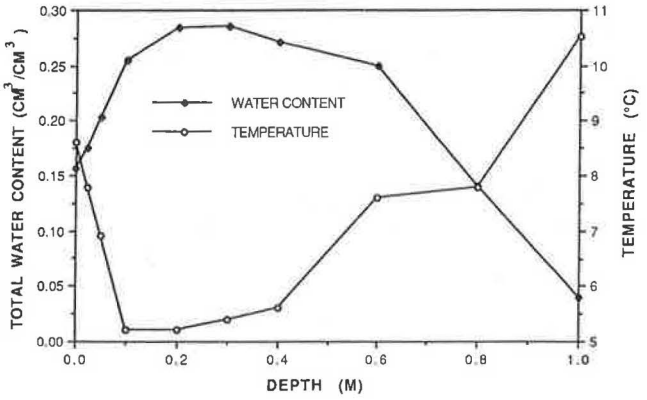

FIGURE 2 Initial water content and temperature profile on November 5, 1989, at the field site.

temperature and soil water content for Run 1 are shown in Figure 3.

Soil properties data required by the SHAW model are profiles of properties including soil texture, dry bulk density, water retention curve parameters, and saturated hydraulic conductivity. Soil texture data and soil bulk density data were measured directly from soil samples. The procedures for estimating soil hydraulic and thermal properties from texture and bulk density data are described in the following paragraphs.

The total porosity of the soil was estimated by assuming a particle density of 2.65 g/cm^3. The soil hydraulic parameters including pore size distribution index b, air entry potential Ψ_e, and saturated hydraulic conductivity K_S were estimated from soil bulk density and soil texture. Campbell (*32*) presented empirical equations for calculating b, Ψ_e, and K_S on the basis of the geometric mean particle size, d_g (mm), and geometric standard deviation, σ_g (mm). These geometric properties were calculated from the following equations.

$$d_g = \exp(x) \tag{3}$$

and

$$\sigma_g = \exp(y) \tag{4}$$

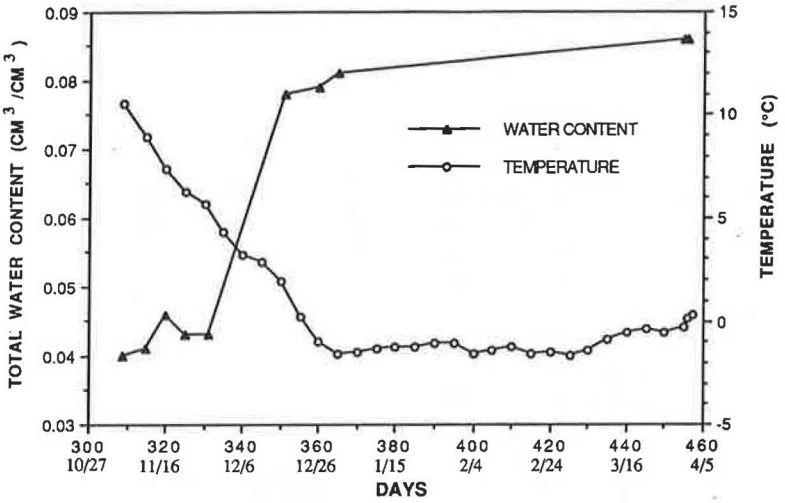

FIGURE 3 Temperature and total water content specified at the lower boundary of 1-m depth for the SHAW model simulations.

in which

$$x = m_c \ln(0.001) + m_{si} \ln(0.026) + m_{sa} \ln(1.025) \quad (5)$$

$$y = [m_c(\ln 0.001)^2 + m_{si}(\ln 0.026)^2 + m_{sa}(\ln 1.025)^2 - x^2]^{1/2} \quad (6)$$

and m_c, m_{si}, and m_{sa} are the mass fractions of clay, silt, and sand, respectively.

With these parameters, the pore size distribution index b can be calculated from

$$b = -2\Psi_{es} + 0.2\sigma_g \quad (7)$$

where

$$\Psi_{es} = -0.5 d_g^{-1/2} \quad (8)$$

The equations from Campbell (*32*) for estimating air entry value and saturated hydraulic conductivity are as follows:

$$\Psi_e = \frac{\Psi_{es}}{g}\left(\frac{\rho_b}{1.3}\right)^{0.67b} \quad (9)$$

$$k_s = 14.4\left(\frac{1.3}{\rho_b}\right)^{1.3b} \exp[-(6.9m_c + 3.7m_{si})] \quad (10)$$

where

Ψ_e = air entry value, m;
ρ_b = bulk density, g/cm³;
g = acceleration of gravity, 9.8 m/sec²; and
K_s = saturated hydraulic conductivity, cm/hr.

On the basis of these equations, the soil parameters for hydraulic properties were calculated and are presented in Table 1. This table includes two sets of parameters for pore size distribution, air entry potential, and saturated hydraulic conductivity. One set was calculated from Equation 8, which has a coefficient of −0.5. The other set was calculated from the same equation but with a coefficient of −0.2, which was used by Flerchinger (*14*). Both sets of soil parameters were used for input to the SHAW model.

TABLE 1 MEASURED AND ESTIMATED PROPERTIES FOR THE SOIL AT THE EXPERIMENTAL SITE LOCATED AT THE ROSEMOUNT EXPERIMENT STATION

Depth (cm)	ρ_b (g/cm³)	Sand	Silt	Clay	b*	Ψ_e^* (cm)	K_s^* (cm/h)	b#	$\Psi_e^\#$ (cm)	$K_s^\#$ (cm/hr)
2.5	1.016	0.19	0.58	0.23	8.24	-8	4.82	4.42	-6	1.42
5.0	1.012	0.19	0.58	0.23	8.24	-8	5.03	4.42	-6	1.45
10.0	1.112	0.19	0.58	0.23	8.24	-14	1.83	4.42	-8	0.84
20.0	1.204	0.19	0.58	0.24	8.44	-22	0.75	4.49	-11	0.50
30.0	1.270	0.15	0.64	0.22	8.41	-31	0.38	4.29	-13	0.34
40.0	1.261	0.15	0.64	0.22	8.41	-29	0.41	4.29	-13	0.35
60.0	1.275	0.19	0.59	0.22	8.09	-29	0.44	4.33	-12	0.40
80.0	1.345	0.31	0.50	0.19	7.07	-29	0.45	4.20	-11	0.51
100.0	1.536	0.25	0.57	0.18	7.20	-60	0.11	4.05	-17	0.21

The SHAW model evaluates the thermal conductivity of the soil on the basis of the de Vries (*32*) equation, which can be written as,

$$\lambda = \frac{\sum \zeta_j \lambda_j V_j}{\sum \zeta_j V_j} \quad (11)$$

where

ζ_j = weighting factor for the jth soil constituent,
λ_j = thermal conductivity of the jth soil constituent, and
V_j = volumetric fraction of the jth soil constituent.

For the thermal conductivity of soil minerals, the value of 7.5 was used on the basis of a weighted average of approximately 78 percent quartz (sand and silt) with a thermal conductivity of 8.8 W/m-°C, and 22 percent clay minerals with a thermal conductivity of 2.9 W/m-°C. The thermal conductivity of water, ice, and air were taken as 0.57, 2.2, and 0.025 W/m-°C, respectively (*29*). The weighting factors were determined as 0.20 for soil solids, 1.0 for water, 0.51 for ice, and

1.47 for air, based on de Vries (*33*), by assuming spherical solid particles.

Hypothetical Paved Condition

The only difference between the paved and the unpaved soil condition is the presence of the base coarse material and the pavement. For the pavement condition, the concrete pavement is 25 cm thick and the base coarse material is 15 cm thick. The soil below the base coarse material is the same soil present in the unpaved soil at the depth of 40 cm and below. The bulk density of the concrete is taken as 2.30 g/cm^3 and the saturated hydraulic conductivity is assumed to be 0.001 cm/hr. The albedo of the concrete is prescribed as 0.20. For the base coarse material, the bulk density is prescribed as 1.8 g/cm^3 and the saturated hydraulic conductivity is 1.8 cm/hr. The temperature at the lower boundary of 10-m depth is specified as 5.6°C and the soil water content is specified as 0.3.

RESULTS AND DISCUSSION

The primary interest of the current modeling exercise is in testing the ability of the SHAW model to predict observed liquid soil water content and soil temperature profiles. Therefore, solute transport in the soil is not considered although the SHAW model has the facility to predict solute transport. The simulation was started at the date of November 5, 1989, and ended on March 31, 1990, the period of measured data. Simulations were performed using both soil parameter data sets presented in Table 1, but only the simulated results from the soil parameter set derived with the Flerchinger (*14*) coefficient are presented because these were in best agreement with field observations.

Run 1

Temperature Profile

The comparison between the measured and predicted field temperature at a depth of 10 cm is shown in Figure 4. Except for large disagreements on Days 318 to 328 and 345 to 358, the measured and predicted temperatures are in good agreement. The lowest temperature is about −14°C for both measured and predicted values. The measured minimum occurs on Day 356, whereas the predicted minimum occurs on Day 351. The predicted temperature values appear to be more responsive to variations in air temperature than the measured temperature, at least for the first part of the period of observation. Fluctuations in both the observed and predicted temperatures appear to be similar after Day 350.

Figure 5 shows the predicted and measured temperature for the 20-cm depth. The overall trend of the temperature variation at the 20-cm depth is similar to that of the 10-cm depth. However, the curves for both predicted and measured temperature have been smoothed and the magnitude of the peaks observed at the 10-cm depth have been reduced at the 20-cm depth. The minimum measured temperature is about

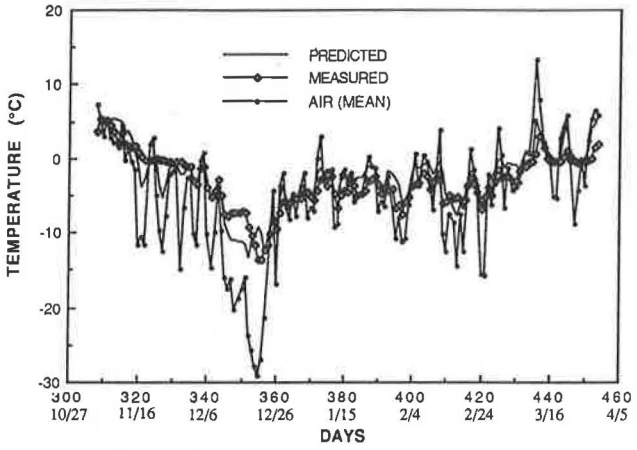

FIGURE 4 Comparison of temperature predicted by the SHAW model with measured temperature at the 10-cm depth.

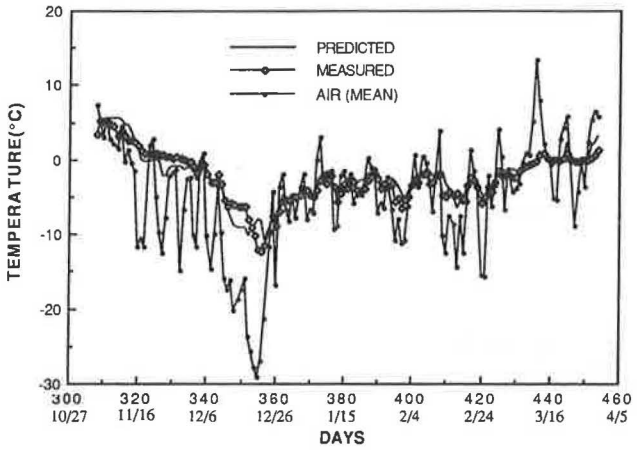

FIGURE 5 Comparison of temperature predicted by the SHAW model with measured temperature at the 20-cm depth.

−12.5°C, which occurs about 2 days later than at the 10-cm depth. The minimum predicted temperature is about −11°C. For the period following the minimum temperature, the predicted and measured temperatures are in good agreement.

The predicted and measured temperatures for the 80-cm depth are shown in Figure 6. Both the predicted and measured temperature variations are smooth. The lowest predicted and measured temperatures are each about −2.8°C. The overall agreement between measured and observed values is good for the entire period of observation. The single low temperature point at Day 365 appears to be an error in the temperature measurement.

Using the SHAW model, Flerchinger (*14*) simulated soil temperature profiles for a conventionally tilled soil with a bare surface, and a no-till soil having a heavy crop residue cover. He compared his predicted results with measured temperatures at the soil surface and at depths of 7.5 and 15 cm. The comparison indicated that the soil temperature predicted at the soil surface and at the two depths agreed well with the measured temperatures. The results presented from this study confirm the results given by Flerchinger (*14*) and demonstrate that the SHAW model has a good capability for predicting soil temperature profiles.

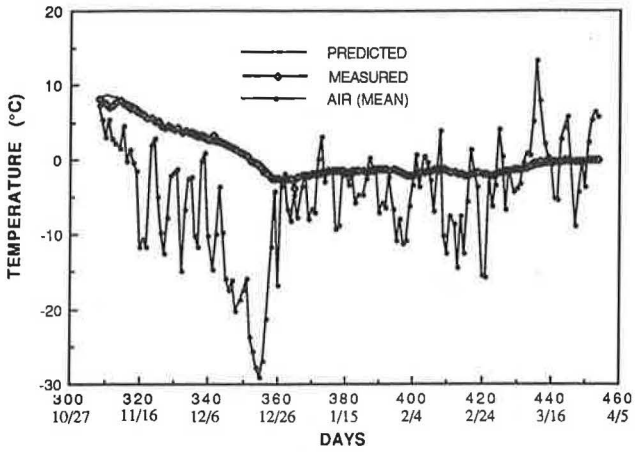

FIGURE 6 Comparison of temperature predicted by the SHAW model with measured temperature at the 80-cm depth.

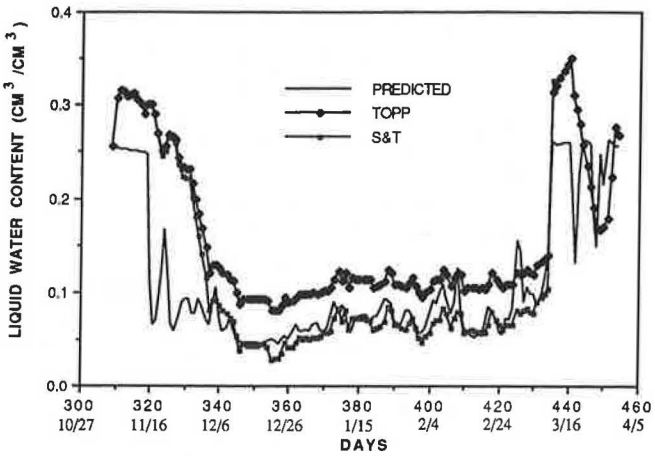

FIGURE 7 Comparison of liquid soil water content predicted by the SHAW model with measured liquid soil water content at the 10-cm depth.

Liquid Soil Water Content Profile

The model output results give the total water content and ice content. For comparison with the measured liquid soil water content data, the predicted liquid soil water content was obtained by subtracting the predicted ice content from the predicted total water content. The predicted liquid soil water content at depths of 10, 20, and 80 cm are plotted with the measured field data in Figures 7–9, in which the measured data are shown as sets labeled TOPP and S&T. The TOPP data were derived using the calibration equation from Topp et al. (*30*) to convert measured TDR dielectric constant with liquid soil water content. The Topp et al. calibration was developed for unfrozen soils but was assumed here to apply for frozen soil conditions. The S&T data were derived using the calibration equation from Smith and Tice (*31*) developed for frozen soil conditions. The largest difference between the two calibration equations occurs for liquid soil water contents below 0.10.

For the liquid soil water content at the 10-cm depth, Figure 7 shows that the predicted liquid soil water content agrees very well with the S&T data from Day 336 to Day 435 when most soil water is frozen. The TOPP data are underpredicted for this same period. The predicted liquid soil water content is lower than the measured content right after the beginning of the simulation. This difference may have been caused by an error in the precipitation record at the site. The precipitation record for the second two days of the simulation were missing. The observed soil water content indicates that a precipitation event may have occurred on the second day of the simulation. It can be seen that the predicted freezing for the 10-cm depth occurs around Day 316 and the measured data show freezing occurs around Day 320. The delay in observed initial freezing is because of the higher liquid soil water content.

The time of thawing observed is similar to the predicted time of thawing in which liquid soil water content suddenly increased a significant amount. However, for the time after Day 435 the measured liquid soil water content is increased to about 0.36, whereas predicted liquid soil water content is increased to 0.26. Several freezing and thawing cycles can be

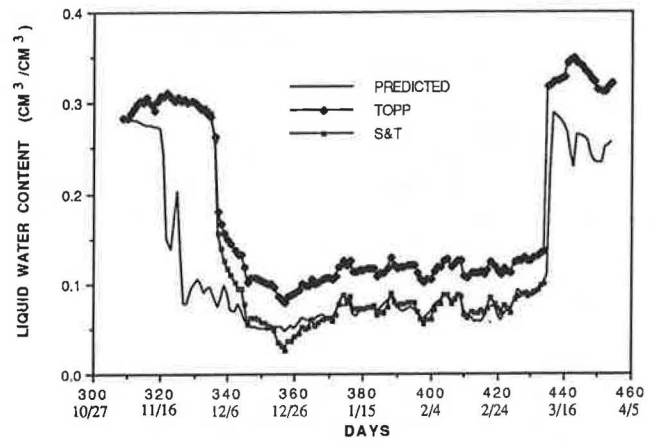

FIGURE 8 Comparison of liquid soil water content predicted by the SHAW model with measured liquid soil water content at the 20-cm depth.

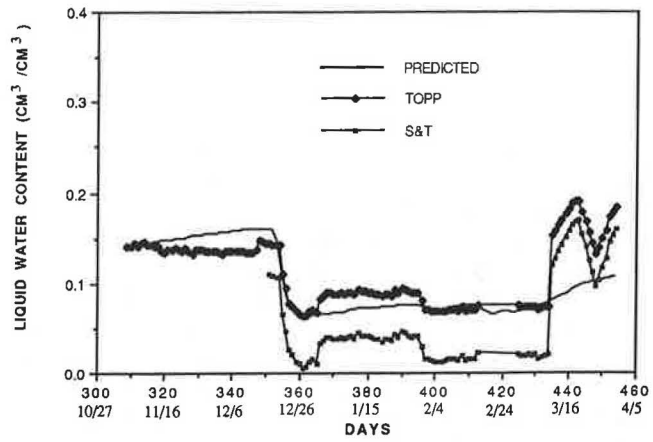

FIGURE 9 Comparison of liquid soil water content predicted by the SHAW model with measured liquid soil water content at the 80-cm depth.

clearly seen from predicted liquid soil water contents, which correspond to the change of air temperature. The measured data seem less sensitive to the fluctuation of the air temperature. This is probably caused by the additional heat capacitance and latent heat associated with the higher water content for the observed data.

Similar to the results for the 10-cm depth, Figure 8 shows that the predicted liquid soil water content at the 20-cm depth agrees very well with the S&T data from Day 340 to Day 435, whereas the TOPP data again lie above the predicted. The predicted liquid soil water content underpredicts the measured liquid soil water content before freezing, probably for the same reasons given earlier for the 10-cm depth. The predicted freezing occurs about 18 days earlier than the measured, again because of the additional liquid soil water in the profile. The time of thawing occurs about the same day for predicted and measured. However, for the time after Day 435 the predicted liquid soil water content is again lower than the measured content.

Figure 9 shows the predicted and measured liquid soil water content at 80 cm. The predicted liquid soil water content agrees fairly well with the TOPP data, but overpredicts the S&T data. A slight increase of water content is observed for the predicted liquid soil water content before freezing, whereas the measured liquid soil water content remained fairly constant for the same time period. The predicted freezing of the soil water at the 80-cm depth occurs at about the same time as the measured. The thawing times for the predicted and the measured are close, but the predicted thawing process is much slower than the measured process. The difference leads to a large difference in liquid soil water content after thawing begins. The fluctuation in the measured liquid soil water content after Day 442 corresponds to the observed air temperature fluctuations.

Flerchinger (*14*) compared the total soil water content predicted with the SHAW model to measured data total soil water content data for a soil profile up to a 170-cm depth. The comparisons were made for selected days, not for the entire period as done here. For those selected days, most of the predicted total soil water content profiles were observed to agree well with the measured data. However, significant differences between predicted and measured total soil water contents were also found on some of the selected days.

Frost and Thaw Depth

Because no direct measurement of frost and thaw depth was made, the actual frost and thaw depth was estimated from the measured liquid soil water content and temperature profile data. The soil was considered frozen at a given depth when the temperature at that depth fell below 0°C and the liquid soil water content at that depth exhibited a sudden drop. An exact measure of the maximum depth of frost penetration could not be made because the temperature and soil water content sensors were not closely spaced, and only existed down to the 1-m depth. Based on this field data, it is estimated that the maximum frost depth over the entire winter period was about 1 m. The predicted maximum depth is 92 cm.

The comparison of predicted and measured frost and thaw depth can be seen from Figure 10. It is seen that the predicted

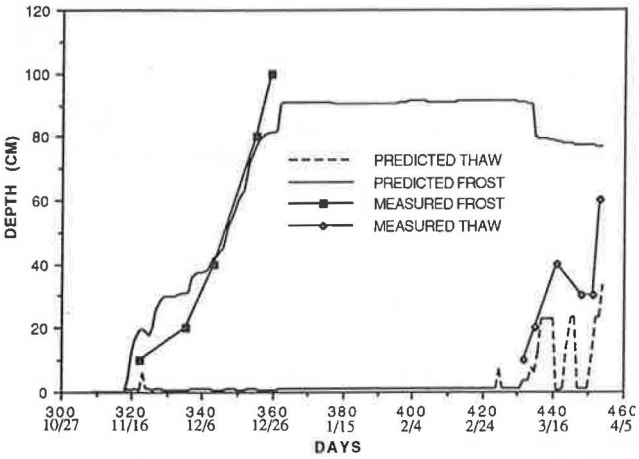

FIGURE 10 Comparison of frost-thaw depth predicted by the SHAW model with measured frost-thaw depth.

frost depth agrees well with measured data up to Day 355. The largest difference between predicted and measured frost depth occurs between Days 320 and 342 when the predicted frost depth advances faster than the measured frost depth over the depth from 10 to 20 cm. On day 360, both the predicted and the measured frost depths reached maximum values. However, the predicted maximum frost depth is about 8 cm less than the measured maximum frost depth.

The predicted thawing started from Day 430, which is about the same time as the initiation of thawing estimated from the measured data. Because of the cycling between the cold and warm weather, there are several thaw and freezing cycles. The measured data indicate that the whole soil profile thawed completely on Day 455. However, model prediction indicated that thawing was not complete until about 4 days later.

Flerchinger (*14*) simulated the frost depth for six field plots for two winter periods. Surface cover conditions applied to the plots included bare, light, medium, and heavy crop residue amounts. The simulated results were compared to the frost depth estimated by electrical resistance blocks and frost tube methods. For most of these stimulations, the predicted frost depths were generally midway between the frost depths estimated by the resistance block and frost tube data. This indicated a reasonable agreement between predicted and measured frost depth. However, disagreement was found in some cases. For instance, the predicted frost depths were slightly larger than the measured frost depth for two of the plots having a medium and heavy residue cover, whereas the predicted frost depth was lower than measured frost depth for one of the plots having light residue cover.

Flerchinger and Hanson (*34*) applied the SHAW model to a rangeland watershed. The simulation was performed for three sites through the 1986–1987 winter, and one site through the two-winter period of 1985–1987. The results exhibited good agreement between predicted and measured temperatures at depths of 2.5, 5, and 10 cm. The predicted maximum frost depth generally agreed with measured values within less than a 10 percent error. For one site, a 14 percent difference between the predicted and measured maximum frost depth was found. Soil water content prediction results were not provided.

Runs 2 and 3

Effect of Pavement

For the comparison of frost-thaw depth between the unpaved and paved soil profile, the results of Runs 2 and 3 are plotted in Figure 11. The frost and thaw depth for the paved surface is measured relative to the surface of the pavement. The frost penetration is deeper in the paved profile than in the unpaved profile for the winter period examined here. Initiation of soil freezing occurs on Day 318 for both the paved and unpaved soil profiles. However, the frost penetration advances rapidly in the paved profile in contrast to the unpaved profile. It only takes 4 or 5 days for the top 40 cm of the paved soil to freeze (concrete and base coarse), whereas it requires about 30 days for the same depth of soil freezing to occur in the unpaved soil profile. This is because the concrete and base coarse material in the paved site have larger thermal conductivity than the top 40 cm of soil and because the concrete and the coarse material freezing release less latent heat because of the low moisture content in the concrete and low soil water content of the coarse base.

There is a short period of about 20 days after the top 40-cm depth freezes in the paved profile in which the freezing depth remains relatively constant while the advancement of frost depth continues in the unpaved profile. This is because of relatively high initial soil water content around 0.26 at the depth of 40 to 60 cm in the paved profile and because freezing induces the upward flow of water to the freezing front. Then the frost depth advances consistently to the maximum depth of 80.2 cm in the paved profile near Day 357. A similar trend in frost penetration is seen for the unpaved profile after Day 340; however, the maximum frost depth is 61 cm on Day 360.

The simulation results of thaw depth response indicate that the thaw depth in the paved profile is significantly larger than that in the unpaved profile for several warm periods. The reason for the higher thaw depth response for the paved soil profile in comparison to the unpaved profile is the same given earlier for frost depth response.

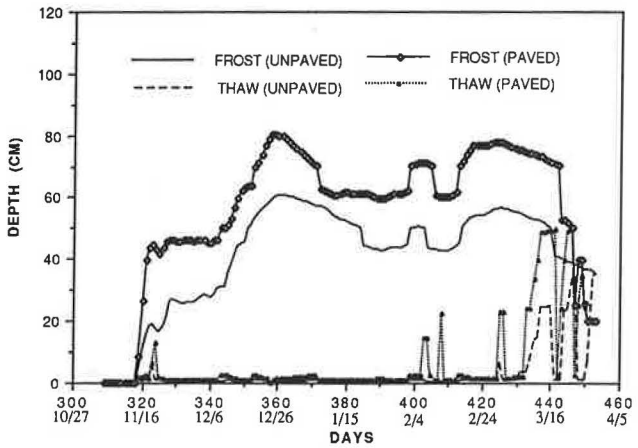

FIGURE 11 Comparison of frost-thaw depth predicted by the SHAW model for two hypothetical cases; the case of a bare soil surface and the case of a paved soil surface. (For both cases, the lower boundary conditions were specified as constant temperature and constant total water content at a depth of 10 m.)

SUMMARY AND CONCLUSION

The SHAW model has been tested with measured liquid soil water content and temperature data acquired over the winter of 1989 for a field site located at Rosemount, Minnesota. Very good agreement was observed between the predicted and measured soil temperature profiles, and good agreement was found between the frost depth estimated from the field data and the frost depth predicted by the model. Observed thaw depth response was predicted somewhat less satisfactorily by the SHAW model, although the model did accurately predict the initiation of the major thaw event.

Good agreement between measured and predicted liquid soil water content depended on the calibration equation used to convert TDR dielectric measurements to liquid soil water content values. The calibration equation of Smith and Tice (*31*) yielded better agreement for depth less than 80 cm, while the calibration equation of Topp et al. (*30*) yielded better agreement for a depth of 80 cm. Additional future work is needed to assess the calibration equation for TDR measurements for variably saturated, variably frozen soils.

In addition to needing more accurate liquid soil water content measurements, improving agreement between predicted and measured liquid soil water content requires having better-defined soil hydraulic properties for variably saturated, variably frozen soil conditions. In this study, these properties were not measured directly for either unfrozen or frozen soil conditions, but were instead derived from estimates using equations based on measured grain size distribution and bulk density of the soil. Additional work is needed to measure these properties directly.

It is unlikely that disparities between measured and predicted liquid soil water content can be attributed to limitations of the mathematical equations on which the SHAW model is based. However, this possible source of inaccuracy will be assessed in future studies.

After testing the SHAW model with measured field data, the effects of concrete pavement and a layer of base coarse on frost and thaw penetration into the soil profile were assessed. This assessment was done by comparing frost-thaw response for a paved soil and an unpaved soil. Results indicated that the frost-thaw response is more rapid and of greater magnitude for the paved soil case than for the unpaved case.

The SHAW model was originally intended to solve coupled water flow and heat transport problems for conditions commonly found in agricultural, forested, and range lands. These conditions typically have a soil surface covered with vegetation and residue in addition to snow. However, the SHAW model facilitates the simulation of layered media by allowing the assignment of appropriate hydraulic and thermal properties to each layer. It was therefore possible to simulate the presence of a paved surface by assigning hydraulic and thermal properties for concrete to the top layer of the profile. Preliminary analysis indicates that the SHAW model has the potential to be a useful tool to adequately predict the status of soil water and soil heat beneath pavements.

ACKNOWLEDGMENT

The authors wish to thank the Center for Transportation Studies at the University of Minnesota and the Minnesota De-

partment of Transportation for financial support of this study, which was published as Paper 18,769 of the scientific journal series of the Minnesota Agricultural Experiment Station on research conducted under Minnesota Agricultural Experiment Station Project 12-48. The authors also wish to thank Gerald N. Flerchinger for providing the SHAW model and for suggestions on running the model.

REFERENCES

1. K. A. Czurda. Freezing Effects on Soils: Comprehensive Summary of the ISGF 82. *Cold Regions Science and Technology*, Vol. 8, 1983, pp. 93–107.
2. B. D. Kay and E. Perfect. *5th International Symposium on Ground Freezing: State of the Art: Heat and Mass Transfer in Freezing Soils*, Jones and Holden (eds.), Balkema, Rotterdam, 1988, pp. 3–21.
3. L. C. Lundin, *Water and Heat Flows in Frozen Soils: Basic Theory and Operational Modeling*. Ph.D. dissertation, Uppsala University, Uppsala, Sweden, 1989.
4. R. L. Harlan. Analysis of Coupled Heat-Fluid Transport in Partially Frozen Soil. *Water Resources Research*, Vol. 9, No. 5, 1973, pp. 1314–1323.
5. G. F. Kennedy and J. Lielmezs. Heat and Mass Transfer of Freezing Water-Soil System. *Water Resources Research*, Vol. 9, No. 2, 1973, pp. 395–400.
6. B. D. Kay and P. H. Groenevelt. On the Interaction of Water and Heat Transport in Frozen and Unfrozen Soils, I. Basic Theory: The Vapor Phase. *Soil Science Society of America Proceedings*, Vol. 38, 1974, pp. 395–400.
7. P. H. Groenevelt and B. D. Kay. On the Interaction of Water and Heat Transport in Frozen and Unfrozen Soils, II. The Liquid Phase. *Soil Science Society of America Proceedings*, Vol. 38, 1974, pp. 400–404.
8. G. L. Guymon and J. L. Luthin. A Coupled Heat and Moisture Transport Model for Arctic Soils. *Water Resources Research*, Vol. 10, 1974, pp. 995–1001.
9. Y. W. Jame and D. I. Norum. Heat and Mass Transfer in a Freezing Unsaturated Porous Medium. *Water Resources Research*. Vol. 16, 1980, pp. 811–819.
10. T. V. Hromadka II, G. L. Guymon, and R. L. Berg. Some Approaches to Modeling Phase Change in Freezing Soils. *Cold Regions Science and Technology*, Vol. 4, 1981, pp. 137–145.
11. G. L. Guymon, T. V. Hromadka, II, and R. L. Berg. A One Dimensional Frost Heave Model Based Upon Simultaneous Heat and Water Flux. *Cold Regions Science and Technology*, Vol. 3, 1980, pp. 253–262.
12. S. K. J. Kung and T. S. Steenhuis. Heat and Moisture Transfer in A Partly Frozen Nonheaving Soil. *Soil Science Society of America Journal*, Vol. 50, 1986, pp. 1114–1122.
13. S. Mu and B. Ladanyi. Modeling of Coupled Heat, Moisture and Stress Field in Freezing Soil. *Cold Regions Science and Technology*, Vol. 14, 1987, pp. 237–246.
14. G. N. Flerchinger, *Simultaneous Heat and Water Model of A Snow-Residue-Soil System*. Ph.D. dissertation, Washington State University, Pullman, 1987.
15. G. N. Flerchinger and K. E. Saxton. Simultaneous Heat and Water Model of A Freezing Snow-Residue-Soil System. 1. Theory and Development. *Transactions of the ASAE*, Vol. 32, 1989, pp. 573–578.
17. J. L. Pikul, L. Boersma, and R. W. Rickman. Temperature and Water Profiles During Diurnal Soil Freezing and Thawing: Field Measurements and Simulation. *Soil Science Society of America Journal*, Vol. 53, 1989, pp. 3–10.
18. J. L. Pikul and J. F. Zuzel. Heat and Water Flux in A Diurnally Freezing and Thawing Soil. In *Proc., International Symposium on Frozen Soil Impacts on Agricultural, Range, and Forest Lands*, K. R. Cooley (ed.), Spokane, Wash., 1990, pp. 113–119.
19. J. L. Pikul and R. R. Allmaras. A Field Comparison of Null-Aligned and Mechanistic Soil Heat Flux. *Soil Science Society of America Proceedings*, Vol. 48, 1984, pp. 1207–1214.
20. A. R. Jumikis. Some Concepts Pertaining to Freezing Soil Systems, In *Special Report* 40: *Water and Its Conduction in Soils*, H. F. Winkerhorn (ed.), National Research Council, Washington, D. C., 1958, pp. 178–190.
21. A. C. Palmer. Ice Lensing, Thermal Diffusion and Water Migration in Freezing Soils. *Journal of Glaciology*, Vol. 6, 1967, pp. 681–694.
22. A. I. Wallace and P. J. Williams. Problems of Building Roads in the North. *Canadian Geography Journal*, Vol. 89, No. 1–2, 1974, pp. 40–47.
23. R. L. Berg, G. L. Guymon, and T. C. Johnson. *Mathematical Model to Correlate Frost Heave of Pavements With Laboratory Predictions*. Report 80-110. U.S. Army Cold Regions Research and Engineering Laboratory, Hanover, N.H., 1980.
24. R. D. Miller, Freezing Phenomena in Soils. In *Applications of Soil Physics*, D. Hillel (ed.), Academic Press, New York, 1980, pp. 254–299.
25. M. W. Smith and A. Tvede. The Computer Simulation of Frost Penetration Beneath Highways. *Canadian Geotechnical Journal*, Vol. 14, 1977, pp. 167–179.
26. J. R. Philip and D. A. de Vries. Moisture Movement in Porous Materials Under Temperature Gradients. *Transaction of the American Geophysical Union*, Vol. 38, 1957, pp. 222–232.
27. D. A. de Vries. Simultaneous Transfer of Heat and Moisture in Porous Media. *Transactions of the American Geophysical Union*, Vol. 39, 1958, pp. 909–916.
28. S. A. Taylor and J. W. Cary. Linear Equations for Simultaneous Flow of Matter and Energy in a Continuous Soil System. *Soil Science Society of America Proceedings*, Vol. 28, 1964, pp. 167–172.
29. D. Hillel. *Fundamentals of Soil Physics*, Academic Press, New York, 1980, pp. 287–317.
30. G. C. Topp, J. L. Davis, and A. P. Annan. Electromagnetic Determination of Soil Water Content: Measurements in Coaxial Transmission Lines. *Water Resources Research*, Vol. 16, No. 3, 1980, pp. 574–582.
31. M. W. Smith and A. R. Tice. Measurement of the Unfrozen Water Content of Soils: Comparison of NMR and TDR Methods. Report 88-18. U.S. Army Cold Region Research and Engineering Laboratory, Hanover, N.H., 1988.
32. D. S. Campbell. *Soil Physics With Basic: Transport Models for Soil-Plant Systems*. Elsevier Soil Publishing Co., Amsterdam, The Netherlands, 1985.
33. D. A. de Vries. Thermal Properties of Soils. In *Physics of Plant Environment*, W. R. van Wijk (ed.), North-Holland, Amsterdam, The Netherlands, 1963, pp. 210–235.
34. G. N. Flerchinger and C. L. Hanson. Modeling Soil Freezing and Thawing on a Rangeland Watershed. *Transactions of the ASAE*, Vol. 32, 1989, pp. 1551–1554.

Publication of this paper sponsored by Committee on Frost Action.